

**Pre-Equilibrium Cross Section
Calculations with a realistic
Effective Nucleon-Nucleon Interaction**



Thesis submitted in partial fulfilment of the requirements
for the M.Sc. degree in the Department of Physics at the

University of the Western Cape

Supervisor: **Prof. R. Lindsay**

Co-supervisor: **Dr. A. Green**

November 1998



Declaration

UNIVERSITY *of the*
WESTERN CAPE

I declare that the *Pre-equilibrium Cross Section Calculations with a realistic Effective Nucleon-Nucleon Interaction* is my own work and that the sources I have used or quoted have been indicated and acknowledged by means of complete references.

Acknowledgements

I would like to thank the following people who helped bring this thesis to completion and also those who assisted me throughout my academic career.

My mother, **Aisha Karriem**, for all her love, encouragement, understanding, the prayers and all the **sacrifices** she made for me in the hardest of times.

My supervisor, **Prof. Robert Lindsay** for accepting me as his student and also for all the countless enlightening discussions we've had in my undergraduate years. His friendship, honesty and most importantly, helping me make sense of theoretical nuclear physics, for all the advice he gave, as well as the financial support throughout the years of being a student.

My co-supervisor, **Dr. Andrew Green**, for all his contributions to my understanding of the experimental aspects of nuclear physics. His thought provoking questions, which led to further brain storming and understanding.

Prof. John F. Sharpey-Schafer, who has had a profound impact on my life. An amazingly kind and hard-headed man, who's insight into life and physics is truly unique and who has a special gift of sharing this with others. His criticism, though offending at times, was greatly appreciated and has changed my views about life and physics. I would also like to thank him for the opportunity of working at the National Accelerator Centre, while still completing this work.

The staff of the National Accelerator Centre, especially **Dr. Richard Newman** for showing me how to find my way around the VAX. It certainly played a vital role in all the calculations performed for this thesis as well as the completion of this work.

Dr. Ravi Babu, for his discussions concerning the application of Quantum Mechanics in nuclear physics.

Dr. Greg C. Hillhouse, who always managed to inject some of his endless enthusiasm into my approach to nuclear physics as well as the vacation work in my undergraduate years.

Mr. Elton van Oordt, for being a friend and for writing and assisting me in writing additional computer programmes that enabled me to perform the calculations more efficiently.

Abstract

The principle aim of this work is to improve the way in which pre-equilibrium double differential cross-sections are currently calculated [1, 2, 3, 4]. The theoretical basis for these calculations is the Multistep Direct Theory by Feshbach, Kerman and Koonin (FKK theory) [5]. This theory leads to the simplification of multistep reactions as a folding of single-step reactions through the implementation of the Distorted Wave Born Approximation (DWBA). The pre-equilibrium cross-sections are subsequently calculated with a multistep direct code.

The primary improvement is the use of a realistic effective Nucleon-Nucleon (N-N) interaction in the DWBA code. This is implemented by using DW91N, a DWBA code that is able to accept a more complex effective interaction. The effective interaction used is that of Amos *et al.* [6]. The multistep direct code by Bonetti *et al.* [7] has been modified to distinguish between proton and neutron excitations in the nucleus.

Most previous calculations have used a simple Yukawa interaction of range 1 fm and variable interaction strength V_0 [1]. The interaction strength is usually adjusted to obtain a good agreement between the calculation and the measured data. This approach however lacks physical interpretation, which limits the application of the code in terms of experimental predictions.

The calculations performed are for the (p, p') reaction of 200 MeV protons on ^{90}Zr . The predicted results were compared to data obtained for this reaction by Richter *et al.* [2]. Initial multistep calculations with the realistic effective interaction showed an overprediction of the double differential cross-sections when compared to the data. For this reason it was decided to consider only the first stage of the multi-step reaction. The first stage of the reaction normally contributes most of the cross-section at low excitation energies[2] and in the forward direction.

The results for the first-step calculation show an overprediction in the cross-section with the implementation of the parameter-free N-N interaction. In an effort to improve the agreement between data and calculational prediction, the nuclear model employs an overprediction of the data, but also indicate that it may be improved by considering the way in which nucleus can become excited.

Contents

1	Introduction	1
1.1	Nuclear Reactions	2
1.2	Classification of Reactions	3
1.3	Information from experiments	5
1.4	Aims of this study	7
2	Scattering Theory	8
2.1	Introduction	8
2.1.1	The Quantum Description	10
2.2	Formal Scattering Theory	12
2.2.1	Definitions and notations	12
2.2.2	The Total Wavefunction	13
2.3	The Transition Amplitude	16
2.4	Distorted Waves	20
2.5	The Distorted Wave Born Approximation	24



A Sample input files	74
A.1 .CNF configuration file	74
A.2 .MSD91 input file	76
A.3 .DW91 input file.	79
A.4 .MUDIR file	83



UNIVERSITY *of the*
WESTERN CAPE

Chapter 1

Introduction

Pre-Equilibrium reactions are of great importance to our understanding of nuclear physics. In this thesis a small part of this vast field is addressed. The work is mainly theoretical in nature. I have however attempted to make, in my opinion, important connections between theory and experiment.

Chapter 1 deals with basic concepts from an experimental point of view. In chapter 2 the main theoretical ideas involved in scattering theory are discussed. The FKK theory is introduced in Chapter 3 and the main expressions needed to gain insight into this theory are given.

Chapter 4 outlines the computational details of the calculations and results. Chapter 5 is the concluding chapter which summarises final results and outlines possible further points of investigation.

The measured quantity in any experiment is the energy spectrum, Fig. 1.2. This data is then analysed to obtain the differential cross-sections, commonly referred to as the *cross-section*. The cross-section can be defined as the probability for a certain reaction to occur. There are thus many types of cross-sections, each corresponding to a different reaction outcome. Fig. 1.2 shows a schematic energy spectrum at an incident energy of around 50 MeV. It is given as a function of the energy of the scattered particle.

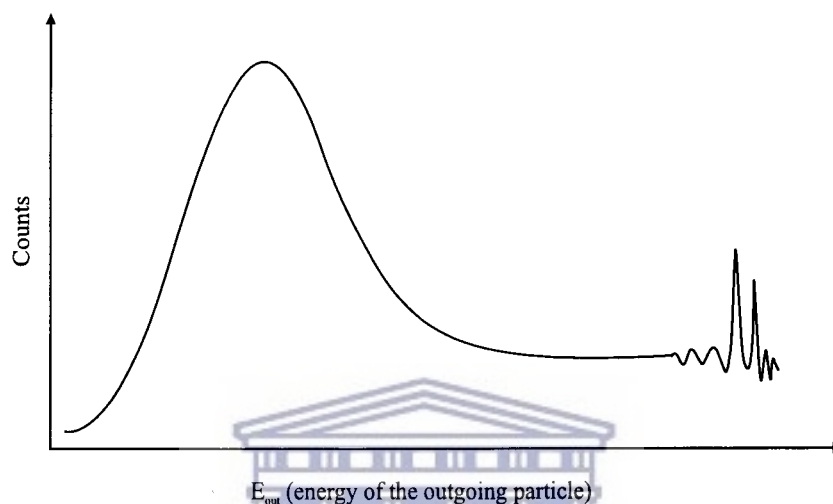


Figure 1.2: Measured energy spectrum.

1.2 Classification of Reactions

During a reaction the target nucleus may become excited as it interacts with the incident particle. The nucleus may be excited in various ways [12]. Fig. 1.3 illustrates the various ways in which the incident particle can interact with the target nucleus for medium energy reactions.

Nuclear reactions are broadly classified as either compound- or direct reactions. In the compound nucleus reactions, the incident particle is captured by the target nucleus and forms a compound nuclear state. The incident particle is absorbed by the nucleus and its energy subsequently distributed among the other nucleons in the target. This leads to the

whereas for compound reactions it takes about 10^{-16} seconds [24].

1.3 Information from experiments

One obtains information about the nucleus by employing theory and experiment. Consider a proton or neutron when it hits the nucleus. The most important property of the incident nucleon that determines the type of reaction is the incident energy. As the incident energy of the particle is increased, so does the nature of the reaction mechanism. The aim is thus to understand this in terms of a simple model from which the cross-sections for various reactions can be calculated. The calculated results are then compared with the experimentally obtained data.

At low energies, protons and neutrons interact very differently with nuclei. This is due to the fact that the neutron has no charge. Protons will be scattered due to the electrostatic repulsion and the cross-section for this process is given by the Rutherford formula [9]

$$\frac{d\sigma}{d\Omega} = \left(\frac{zZe^2}{4\pi\epsilon_0} \right)^2 \left(\frac{1}{4T_a} \right)^2 \frac{1}{\sin^4\left(\frac{\theta}{2}\right)}, \quad (1.1)$$

where

ze = the charge of the projectile

Ze = the charge of the target

T_a = the kinetic energy of the projectile and

θ = the angle of emission.

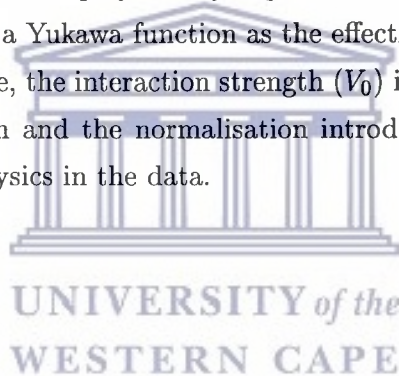
At low energy ($E < 10$ MeV) the proton is unlikely to enter the nucleus. Neutrons on the other hand are able to penetrate the nucleus at these energies and can give rise to compound nucleus formation [12]. As the incident neutron energy increases it results in various nuclear excitations. As soon as a favoured energy level is excited, the cross-section reaches a maximum. These kind of reactions are called resonance reactions.

During this process the incident neutron is absorbed, excites the nucleus and is ejected. By observing the angular distribution of the scattered particles one can extract information about the excited compound nuclear state.

To be able to calculate pre-equilibrium cross-sections are important for various reasons. Looking at Fig. 1.4, one sees that pre-equilibrium reactions contribute to a large portion of the cross section. Indirectly this says that at least half of the possible processes likely to occur for reactions around the 200 MeV region, are pre-equilibrium reactions. The second possible application of being able to calculate these cross sections accurately, is the implementation into radiation transport codes such as MCNP [14]. These type of codes simulate radiation transport and use cross-section data libraries, which form an integral part of the modelling process.

1.4 Aims of this study

The aim of this work is to improve the way pre-equilibrium reaction cross-sections are currently being calculated. More specifically, to improve the interpretation of calculated cross-section results. The N-N interaction plays a very important role in these calculations. Current methods of computations use a Yukawa function as the effective interaction [34]. In order to obtain good fits with this force, the interaction strength (V_0) is adjusted. This approach thus uses a very simple interaction and the normalisation introduces a fitting procedure which may well hide some of the physics in the data.



After the plane waves interacted with the target (considered as a point), one would expect to "see" spherical waves. This treatment is analogous to the scattering of a plane water wave by a point object in the water. The figure below also shows the detector used to detect the reaction products.

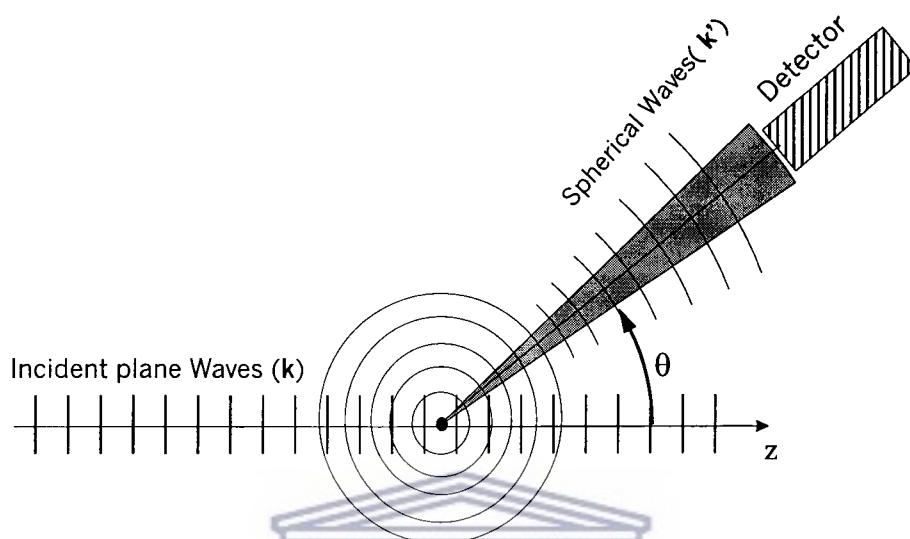


Figure 2.1: Analysis of scattering in terms of plane and spherical waves [29] .



The first term represents the plane wave part and includes the z-co-ordinate only, since the z-co-ordinate is chosen to be parallel to the incident particles momentum (Fig. 2.1). The second term consists of the spherical wave part, $\frac{e^{ikr}}{r}$, and the scattering amplitude $f(\theta, \phi)$. The square of the scattering amplitude [13, 22] is proportional to the probability that the reaction particles are scattered in the direction of (θ, ϕ) . The fact that the scattering potential is considered to be spherically symmetric, eliminates the ϕ -dependence of the scattering amplitude, hence it becomes $f(\theta)$.

The scattering amplitude is related to the differential cross-section [29] through the following expression:

$$\frac{d\sigma}{d\Omega} \propto |f(\theta)|^2. \quad (2.4)$$

One thus has many types of cross-sections, each of which is related to the corresponding scattering amplitude. The cross-section is the most important measurable quantity for any experiment. The aim of scattering theory is thus to provide us with a framework for formulating solutions to the scattering problem from which the desired cross-sections may be extracted.

In the following section the formal developments of the scattering theory will be outlined. The formalism results in exact expressions, which are often in calculable. The best one can often do is to make some assumptions, which will allow for the simplification of the problem. The assumptions as well as the approximations made are largely dependent on the type of nuclear model employed. These assumptions and approximations will be discussed and the calculable expressions given.

2.2.2 The Total Wavefunction

The wavefunction describing the scattering process is thought to be a complete description, that is, we should in principle be able to extract any information prior to and after scattering. Since the exact form of the wavefunction is not known, it is perhaps appropriate to mention that there are two aspects that need consideration. The one is the relative (spatial) description of the system and the other is the internal nuclear description. Intuitively we can thus say that we are at least looking for a wavefunction that is separable [13] in terms of the above considerations. In order to do this we have to construct suitable operators.

Let us start with the internal nuclear operators. The nucleus is to some extent well described by the Shell Model [9]. Hence the internal Hamiltonian for the nucleus **A** in the entrance channel α as in the previous section is [13]

$$H_A = \sum_{i=1}^A (T_i + U_i) + \sum_{i \neq j} V_{ij}, \quad (2.5)$$

where

$T_i = -\left(\frac{\hbar^2}{2m_i}\right) \nabla_i^2$ = is the kinetic energy operator for the i 'th particle,
 $U_i = U(r_i)$ = is a central potential acting on a single nucleon,
 $V_{ij} = V(\mathbf{r}_i - \mathbf{r}_j)$ = is a phenomenological two-body potential, and
 r_i = the co-ordinate of the i 'th particle relative to the nuclear centre.

One may write down similar expressions for the projectile **a**, as well as for particles in the exit channel. The corresponding internal hamiltonians will carry the subscript of the appropriate nucleus.

The complete internal Hamiltonian for the entrance channel α will then be

$$H_\alpha = H_A + H_a. \quad (2.6)$$

The eigenfunctions for H_A and for H_a are denoted by Φ_A and Φ_a respectively. The complete internal wavefunction for the system is then given by

$$\Phi_\alpha = \Phi_a \Phi_A, \quad (2.7)$$

where the various operators were constructed in a similar manner as for channel α . What we thus obtain is

$$\begin{aligned} H &= H_\alpha + T_\alpha + V_\alpha \\ &= H_\beta + T_\beta + V_\beta. \end{aligned} \tag{2.17}$$

The above expression represents what has been said in the introductory quote, i.e. all information about the system is contained in the wavefunction for the system and hence we only need to construct the appropriate operators to extract the required information.



which includes the plane wave solution to the relative part of the wavefunction.

In regions where V_α is not equal to zero we use the method of projection onto a channel. This is done by taking the inner product of Φ_α with Eq.(2.3) and integrating over all internal co-ordinates.

$$\begin{aligned}
\Phi_\alpha^*(E - H_\alpha - T_\alpha)\Psi_\alpha &= \Phi_\alpha^*V_\alpha\Psi_\alpha \\
\Phi_\alpha^*(E\Psi_\alpha - H_\alpha\Psi_\alpha - T_\alpha\Psi_\alpha) &= \Phi_\alpha^*V_\alpha\Psi_\alpha \\
\Phi_\alpha^*E\Psi_\alpha - \varepsilon_\alpha\Phi_\alpha^*\Psi_\alpha - \Phi_\alpha^*T_\alpha\Psi_\alpha &= \Phi_\alpha^*V_\alpha\Psi_\alpha \\
\int E_\alpha(\Phi_\alpha^*\Psi_\alpha) d_{internal} - \int (\Phi_\alpha^*T_\alpha\Psi_\alpha) d_{internal} &= \int (\Phi_\alpha^*V_\alpha\Psi_\alpha) d_{internal} \\
(E_\alpha - T_\alpha) \int (\Phi_\alpha^*\Psi_\alpha) d_{internal} &= \int (\Phi_\alpha^*V_\alpha\Psi_\alpha) d_{internal} \\
(E_\alpha - T_\alpha)(\Phi_\alpha, \Psi_\alpha) &= (\Phi_\alpha, V_\alpha\Psi_\alpha)
\end{aligned} \tag{2.24}$$

The integration co-ordinate, $d_{internal}$, indicates integration over internal nuclear co-ordinates only. The notation $(,)$ indicates this type of integration. The result from the above manipulation yields a solution for the relative wavefunction

$$\psi_\alpha(\mathbf{r}_\alpha) = (\Phi_\alpha, \Psi_\alpha), \tag{2.25}$$

based on the fact that the relative part is independent of the internal co-ordinates.

A solution to the above equation may be obtained by implementing Green's functions methods [29, 22, 17] to obtain a solution of the form

$$\psi_\alpha(\mathbf{r}_\alpha) = \int G_\alpha^0(\mathbf{r}_\alpha, \mathbf{r}'_\alpha)(\Phi_\alpha, V_\alpha\Psi_\alpha) d\mathbf{r}'_\alpha, \tag{2.26}$$

with the following solution

$$G_\alpha^{0(+)}(\mathbf{r}, \mathbf{r}') = \left(\frac{2\mu_\alpha}{\hbar^2} \right) \frac{e^{ik_\alpha|\mathbf{r}-\mathbf{r}'|}}{4\pi|\mathbf{r}-\mathbf{r}'|}. \tag{2.27}$$

The above function describes the source of the potential, in this case the target nucleus. The co-ordinate (\mathbf{r}'_α) refers to region within the nucleus. The plus sign on the Green's function solution and on the relative solution for the wavefunction designates that the spherically scattered waves are radially outgoing. Inserting the above expressions into Eq.(2.26) we obtain the following solution

$$\psi_\alpha(\mathbf{r}_\alpha) = \left(-\frac{\mu_\alpha}{2\pi\hbar^2} \right) \int \frac{e^{ik_\alpha|\mathbf{r}-\mathbf{r}'|}}{|\mathbf{r}-\mathbf{r}'|} (\Phi_\alpha, V_\alpha\Psi_\alpha) d^3r'_\alpha. \tag{2.28}$$

One may obtain the scattering amplitudes for other exit channels in a similar manner by projecting the complete wavefunction onto a certain channel. Consider the channel β for example. The solution of the relative wavefunction will have the following form:

$$\psi_\beta(\mathbf{r}_\beta) = (\Phi_\beta, \Psi_\alpha). \quad (2.35)$$

The α designates the initial state of the system. In exactly the same way we obtain the following solution

$$\psi_\beta^{(+)}(\mathbf{r}_\beta) = -\frac{\mu_\beta}{2\pi\hbar^2} \frac{e^{(-ik_\beta r_\beta)}}{r_\beta} \int e^{(ik_\beta \cdot \mathbf{r})} (\Phi_\beta, V_\beta \Psi_\alpha^{(+)}) d\mathbf{r}, \quad (2.36)$$

and we identify the scattering amplitude as

$$f(\theta) = -\frac{\mu_\beta}{2\pi\hbar^2} e^{(-ik_\beta \cdot \mathbf{r})} (\Phi_\beta, V_\beta \Psi_\alpha^{(+)}) d\mathbf{r}. \quad (2.37)$$

The scattering amplitude in terms of the transition amplitude is

$$f_{\alpha\beta} = -\frac{\mu_\beta}{2\pi\hbar^2} T_{\alpha\beta}, \quad (2.38)$$

with

$$T_{\beta\alpha} = \langle \phi_\beta | V_\beta | \Phi_\alpha^{(+)} \rangle. \quad (2.39)$$

It can thus be seen that the information on the scattering process is contained in the T-matrix elements (transition amplitude).

The asymptotic form of the complete wavefunction can then be written as follows:

$$\Phi_\alpha^+ = \Phi_\alpha \left[e^{i(\mathbf{k}_\alpha \cdot \mathbf{r}_\alpha)} + f_{\alpha\alpha}(\theta) \frac{e^{ik_\alpha r_\alpha}}{r_\alpha} \right] \quad (2.40)$$

$$+ \sum_{\alpha' \neq \alpha} \Phi_{\alpha'} f_{\alpha'\alpha}(\theta) \frac{e^{ik_{\alpha'} r_\alpha}}{r_\alpha} \quad (r_\alpha \rightarrow \infty) \quad (2.41)$$

$$+ \sum_{\beta} \Phi_\beta f_{\beta\alpha}(\theta) \frac{e^{ik_\beta r_\beta}}{r_\beta} \quad (r_\beta \rightarrow \infty). \quad (2.42)$$

Eq.(2.40) is elastic scattering, Eq.(2.41) is inelastic scattering and Eq.(2.42) are other possible reactions.

where χ_α now denotes a solution to the relative part of the wavefunction, since we can write the total wavefunction as $\Psi_\alpha = \chi_\alpha \Phi_\alpha$. Here the Φ_α as before denotes the internal portion of the wavefunction. A solution to the above equation may be obtained in a partial wave expansion in terms of the spherical harmonics to obtain [29]

$$\chi_\alpha^{(+)} = \frac{4\pi}{k_\alpha r_\alpha} \sum_{\ell, m} i^\ell e^{i\sigma_\ell} f_\ell(k_\alpha r_\alpha) Y_\ell^m(\hat{\mathbf{r}}_\alpha) Y_\ell^{m*}(\hat{\mathbf{k}}_\alpha). \quad (2.46)$$

Here the Coulomb interaction has been included by the insertion of the Coulomb phase shift $e^{i\sigma_\ell}$ [28]. The functions f_ℓ are the solutions to the radial Schrödinger equation and are chosen so that the relative wavefunction consists of outgoing spherical waves. These f_ℓ have the following asymptotic form [18]

$$f_\ell(k_\alpha, r_\alpha) = e^{i\delta_\ell} \sin\left(k_\alpha r_\alpha - \frac{\ell\pi}{2} + \delta_\ell\right). \quad (2.47)$$

This equation implies that the only effect the potential has on the radial wavefunction is that it can change its phase δ_ℓ . The subscript ℓ refers to the ℓ 'th partial wave. These wavefunctions may be determined numerically.

The general solution for $\chi_\alpha^{(+)}$ is then

$$\chi_\alpha^{(+)} \rightarrow e^{ik_\alpha \cdot \mathbf{r}_\alpha} + \frac{e^{(ik_\alpha r_\alpha)}}{k_\alpha r_\alpha} \sum_l (2l+1) e^{i\delta_\ell} \sin \delta_\ell P_\ell(\cos\theta). \quad (2.48)$$

One can then also write down the scattering amplitude as

$$f(\theta) = \frac{1}{k_\alpha} \sum_l (2l+1) e^{i\delta_\ell} \sin \delta_\ell P_\ell(\cos\theta). \quad (2.49)$$

Here P_ℓ denotes the Legendre polynomial of order ℓ . The above form (Eq. 2.48) of the relative wavefunction is referred to as spherically distorted waves.

Let us now turn to the situation in which the effective interaction is not zero and we have only the effective interaction present. In this case Eq. (2.44) becomes

$$(E_\alpha - T_\alpha - U_\alpha)\psi_\alpha = (\Phi_\alpha, [V_\alpha - U_\alpha]\Psi_\alpha). \quad (2.50)$$

A solution to the above equation may be obtained in a similar manner in terms of a Green's function such that the general solution to Eq. (2.45) has the the form

$$\psi_\alpha(\mathbf{r}_\alpha) = A\chi_\alpha + \int G_\alpha(\mathbf{r}, \mathbf{r}') [\Phi_\alpha, (V_\alpha - U_\alpha), \Phi_\alpha] d\mathbf{r}', \quad (2.51)$$

What we have achieved up to this point is to separate the potential into two components. This gives rise to the spherical distorted waves which can be calculated by fitting elastic scattering data. These distorted waves serve as the relative solution to the total wavefunction. The next point that is addressed, is the approximation for the total wavefunction, since the above expression still contains the unknown wavefunction Ψ_α .



Let the transferred angular momentum be denoted as follows:

$$\mathbf{j} = \mathbf{J}_B - \mathbf{J}_A \quad (2.61)$$

$$\mathbf{s} = \mathbf{s}_a - \mathbf{s}_b \quad (2.62)$$

$$\mathbf{l} = \mathbf{j} - \mathbf{s}. \quad (2.63)$$

The vector form of the relative angular momentum is denoted by \mathbf{l} , while the quantum number is denoted by ℓ . In the above, \mathbf{j} is the change in the total angular momentum. \mathbf{J}_B and \mathbf{J}_A are the total angular momentum for the particles **B** and **A** respectively. Angular momentum requires that

$$\mathbf{J}_a + \mathbf{J}_A + \mathbf{l}_\alpha = \mathbf{J}_b + \mathbf{J}_B + \mathbf{l}_\beta, \quad (2.64)$$

where \mathbf{l}_α and \mathbf{l}_β denote the relative angular momentum in channel α and β respectively. The matrix element dictates the transition from the initial distorted wave to the final distorted wave. The matrix element may be explicitly written as

$$(\Phi_B \Phi_b | V_\beta - U_\beta | \Phi_A \Phi_a) = (J_B M_B, s_b m_b | V_\beta - U_\beta | J_A M_A, s_a m_a), \quad (2.65)$$

and expanded in terms of the spherical harmonics for the angular momentum transfer

$$\begin{aligned} T_{\beta\alpha}^{DWBA} &= \sum_{\ell s j} (2j+1)^{\frac{1}{2}} \langle J_A j M_A, M_B - M_A | J_B M_B \rangle \\ &\times A_{\ell s j} \beta_{s j}^{\ell m m_b m_a}(\mathbf{k}_\beta, \mathbf{k}_\alpha), \end{aligned} \quad (2.66)$$

where

$$\begin{aligned} \beta_{s j}^{\ell m m_b m_a}(\mathbf{k}_\beta, \mathbf{k}_\alpha) &= \frac{i^{-\ell}}{(2j+1)^{\frac{1}{2}}} \sum_{m'_a m'_b m'} \langle \ell s m', m'_a - m'_b | j m - m_b + m_a \rangle \\ &\times \langle s_a s_b m'_a, -m'_b | s m'_a - m'_b \rangle (-1)^{s_b - m'_b} \\ &\times \int d\mathbf{r}_\beta \int d\mathbf{r}_\alpha \chi_{m'_b m_b}^{(-)*}(\mathbf{k}_\beta, \mathbf{k}_\alpha) f_{\ell s j, m}(\mathbf{k}_\beta, \mathbf{k}_\alpha) \chi_{m'_a m_a}^{(+)*}(\mathbf{k}_\beta, \mathbf{k}_\alpha), \end{aligned} \quad (2.67)$$

with

It is thus clear from this treatment that the cross-section is determined by our model for the nucleus and the effective interaction. The DWBA cross-sections can thus be seen to form a very important part in these calculations.



UNIVERSITY *of the*
WESTERN CAPE

The reason for this is that the FKK involves simpler expressions for calculational purposes. The FKK theory and codes based on this formalism are utilised in this work. Details about these theories and their implementation can be found in [19, 23].

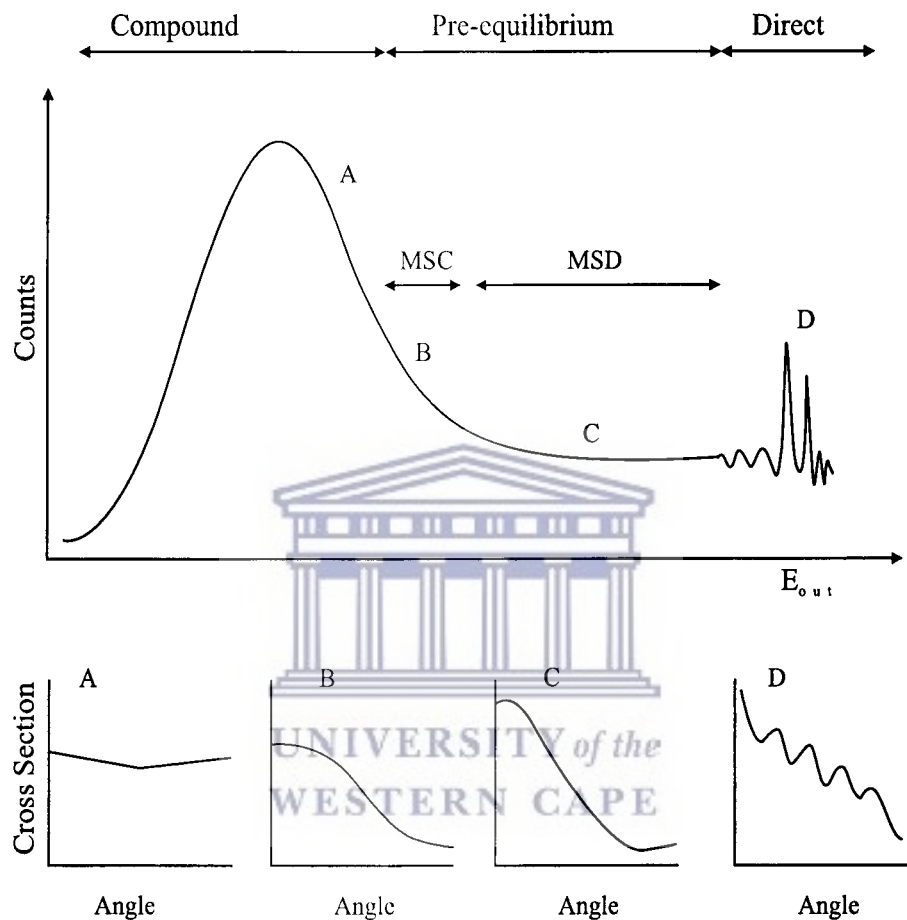


Figure 3.1: Classification of reaction cross-section.

The main ideas in these theories are that the incident projectile undergoes multiple scattering in such a way that it retains a "memory" of the incident channel. Nuclear excitation then proceeds in such a way that the reaction does not evolve to purely compound processes nor is it purely direct in nature. It may be imagined that the incident particle excites the nucleus and is emitted long before the nucleus is fully equilibrated.

3.1.1 Multiple Scattering

The first step toward constructing a suitable model for pre-equilibrium reactions is the idea of multiple scattering. This is not new in any way, but what is different is the mechanism involving nuclear excitation [20, 32]. It is imagined that the nucleus becomes excited through a series of intermediate steps, which involves simple excitations of the nucleus from one step to the next. More complex nuclear excitations are achieved through such a series of simple excitations. The states of highest complexity that can be reached are compound nuclear states. This is illustrated in the figure below.

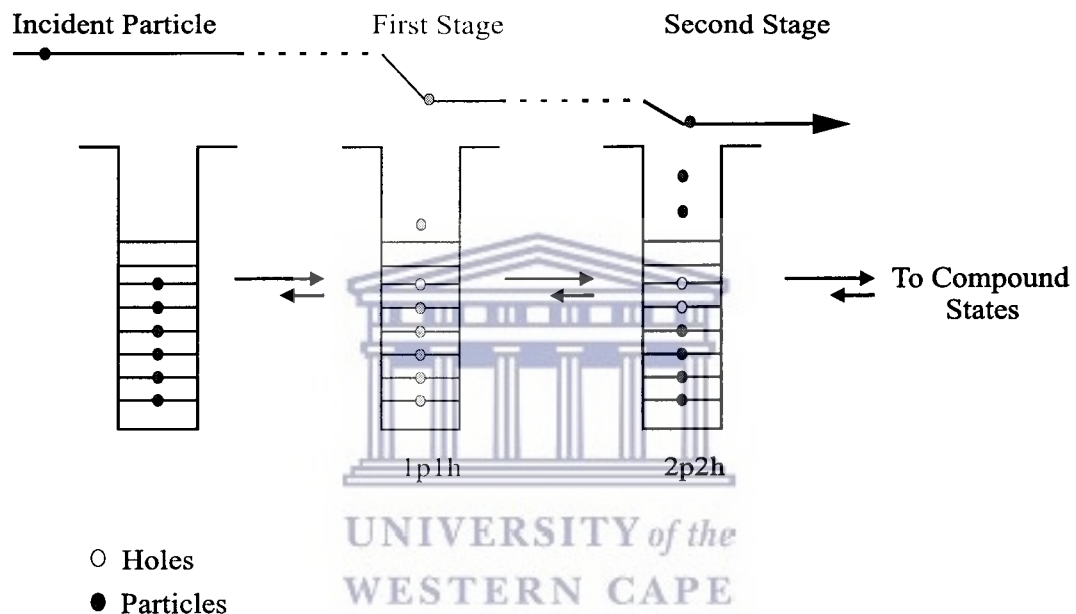


Figure 3.2: Successive excitation in multiple scattering.

As mentioned before, the nuclear model employed in this work is the single-particle shell model. That is, we will be considering the excitation of shell-model states. These states are employed in such a way that when a nucleon is promoted to a higher shell model orbit, it leaves a hole in the orbit from which it originated. The excitations are then referred to as particle-hole excitations as introduced by Griffin [32]. Fig. 3.2 shows the successive excitation of a $1p1h$ and a $2p2h$ state.

Another ingredient of the above picture is that of doorway states [20]. These doorway

3.1.2 Classification of Reactions

If one considers a projectile that interacts with a target nucleus, there is basically one of two things that can occur. The incident particle can cause excitation by becoming bound to the target (Fig. 3.4), or it may excite the nucleus while it is still unbound (Fig. 3.5). The latter is referred to as continuum scattering, which is thought to take place during MSD reactions.

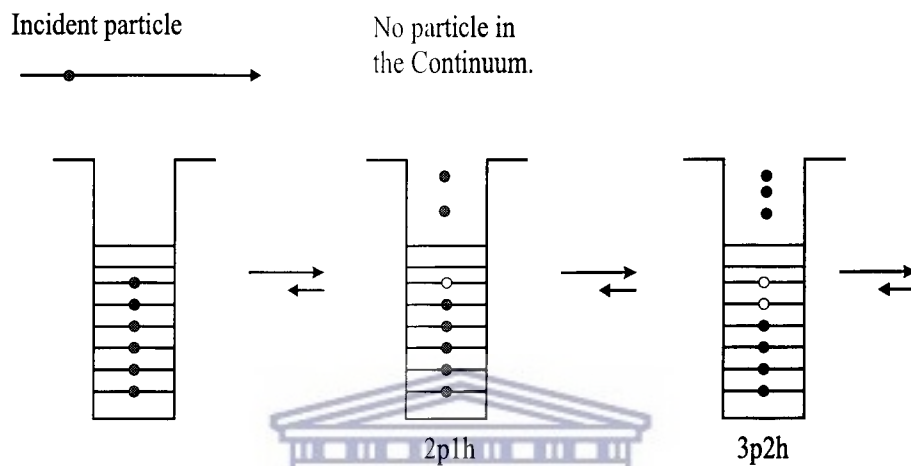


Figure 3.4: Multistep compound reaction.

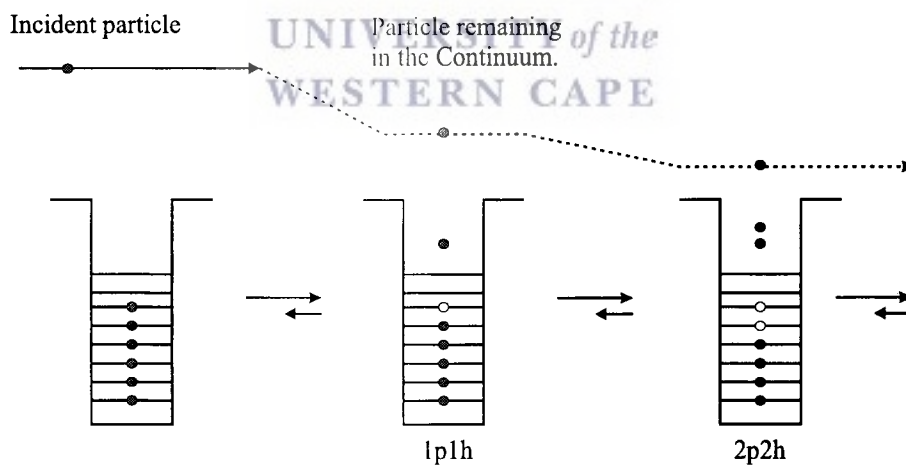


Figure 3.5: Multistep direct reaction.

observes wavefunction interference in cross-sectional data. This effect is always present, since we are dealing with a quantum system. Since the various modes of excitations is so great, the cross-sections resulting from the P-chain for example, can be thought of as being independent and random. This assumption of randomness allows us to calculate the cross-section as a sum of the individual cross-sections without interference.



K_a = is the kinetic energy operator in terms of the relative co-ordinates,
 v_{ia} = the potential between the projectile and the nucleus,
 U_a = the optical potential, and
 V = the residual interaction of the incident nucleon.

The complete Hamiltonian can then be written as

$$H = H_0 + H_1 + h_a + V. \quad (3.6)$$

The shell-model states will be treated as particle-hole states. This would mean that for the shell-model Hamiltonian, these states would satisfy the following relation:

$$H_0|m\mu\rangle = E_{m\mu}|m\mu\rangle, \quad (3.7)$$

where

m denotes the class ($mpmh$)-states,
 μ denotes the configuration of a particular particle-hole state, and
 $E_{m\mu}$ is the energy eigenvalue for a particular state.

The states $|m\mu\rangle$ are pure model states. The real states, as observed experimentally, will be a mixture of these states and will satisfy the following:

$$H_{0+1}|n\rangle = E|n\rangle. \quad (3.8)$$

The state $|n\rangle$ can be expanded in terms of the pure model states as

$$|n\rangle = \sum_{m\mu} a_{m\mu}^n |m\mu\rangle, \quad (3.9)$$

where the $a_{m\mu}^n$ are coefficients denoting the weight of each model state's contribution to the real state. This concludes the internal description of the scattering process. We now turn to the relative description.

The Hamiltonian written down in Eq. (3.2) distinctly depicts expressions for the residual nucleus and the projectile. The description for the projectile is more important than it appears, since it describes the motion of the particle in the continuum. That is, the motion of

3.2.1 The Transition Amplitude

With the above tools we can now consider what happens to a system as it passes through various stages of the reaction. In multiple scattering this is achieved by using the Green's function propagator [22]. The desired information concerning the cross-sections are contained in the T-matrix elements of the reaction. Consider the system in the initial state $|0\rangle|\chi^{(+)}(\mathbf{k}_0)\rangle$ that makes a transition to some final state $|f\rangle|\chi^{(-)}(\mathbf{k})\rangle$. The Born series expansion gives the transition amplitude as

$$T_{f\leftarrow 0} = \langle\chi^{(-)}(\mathbf{k})|\langle f|V + VGV + VGVGV + \dots|0\rangle|\chi^{(+)}(\mathbf{k})\rangle \quad (3.12)$$

$$= \sum_{k=1}^{\infty} T_{f\leftarrow 0}^{(k)}. \quad (3.13)$$

The particle has now been propagated through the target nucleus. $|V|$ corresponds to a single interaction, $|VGV|$ to the second interaction and so on. The index in the summation labels the stage (each step) of the reaction. This would correspond to different energies of the particle in the continuum as it goes from one step to the next. This in turn corresponds to different excitations of the residual nucleus. The Green's function that is employed in the above expression is

$$G = \sum_n \int d\mathbf{k}_1 \frac{|n\rangle|\chi^{(+)}(\mathbf{k}_1)\rangle\langle\hat{\chi}^{(+)}(\mathbf{k}_1)|\langle n|}{E - E_n - E_{k_1} + i\varepsilon}, \quad (3.14)$$

where n labels the intermediate stages. It is important to point out that the above series refers to a process in which one particle remains in the continuum. If at any stage all the particles became bound, then we would have to use the multistep compound reaction formalism.

The final states $|f\rangle$ as in Eq. (3.13) are real states, i.e. those that are experimentally observed. The reason for this is that the Hamiltonian includes H_1 , the residual interaction. In the independent particle model used in the exciton model and in the FKK-theory, the nuclear states used for the experimental states are taken as particle-hole states, which are pure model states. The real nuclear states can be retrieved, by letting $H_1 \rightarrow 0$. In the independent particle model states the coefficients $a_{m\mu}^n$ become $a_{m\mu}^n = \delta_{mn}$ and the final and initial states (Eq. (3.13)) reduce to initial and final particle-hole states. The initial state now becomes $|0\rangle|\chi^{(+)}(\mathbf{k})\rangle$, corresponding to a $0p0h$ state and the final state $|p\nu\rangle|\chi^{(-)}(\mathbf{k})\rangle$, corresponding to $pp\nu h$. The transition amplitude is now

0 = initial state,

$p\nu$ = the final particle-hole state.

The cross-section is usually written down in terms of excitations in a certain energy range rather than discrete excitations. For the real nuclear states we have

$$\frac{d^2\sigma}{d\Omega dE_k} = \sum_f |T_{f\leftarrow 0}|^2 \delta(E_f - E_x). \quad (3.19)$$

Here the delta denotes the energy range of excitation. By putting 3.13 into 3.19 we obtain the following expression:

$$\frac{d^2\sigma}{d\Omega dE_k} = \sum_f \left| \sum_i T_{f\leftarrow 0}^{(i)} \right|^2 \delta(E_f - E_x) \quad (3.20)$$

$$= \sum_i \sum_f |T_{f\leftarrow 0}^{(i)}|^2 \delta(E_f - E_x) + \text{cross terms} \quad (3.21)$$

$$= \sum_i \frac{d^2\sigma^{(i)}}{d\Omega dE_k} + \text{cross terms}, \quad (3.22)$$

which distinguishes between one step ($i = 1$), multistep reactions ($i > 1$) and interference terms. In the case of the independent particle model we have

$$\frac{d^2\sigma}{d\Omega dE_k} = \sum_{p\nu} |t_{p\nu \leftarrow 0}|^2 \delta(E_{p\nu} - E_x), \quad (3.23)$$

and with the never-come-back assumption we get

$$\frac{d^2\sigma}{d\Omega dE_k} = \sum_{p\nu} |t_{p\nu}^{(p)} \leftarrow 0|^2 \delta(E_{p\nu} - E_x). \quad (3.24)$$

The first and second step reaction contribution to the pre-equilibrium cross section will now be written down in terms of the independent particle model, since this is what our calculations are based on.

For the above model we have the t-matrix element as

$$\begin{aligned} t_{1\mu \leftarrow 0} &= t_{1\mu \leftarrow 0}^{(1)} \\ &= \langle \chi^{(-)}(\mathbf{k}) | \langle 1\mu | V | 0 \rangle \hat{\chi}^{(+)}(\mathbf{k}_0) \rangle, \end{aligned} \quad (3.25)$$

3.3 Statistical Averaging

The results obtained from Koning's work can be outlined in the following diagram.

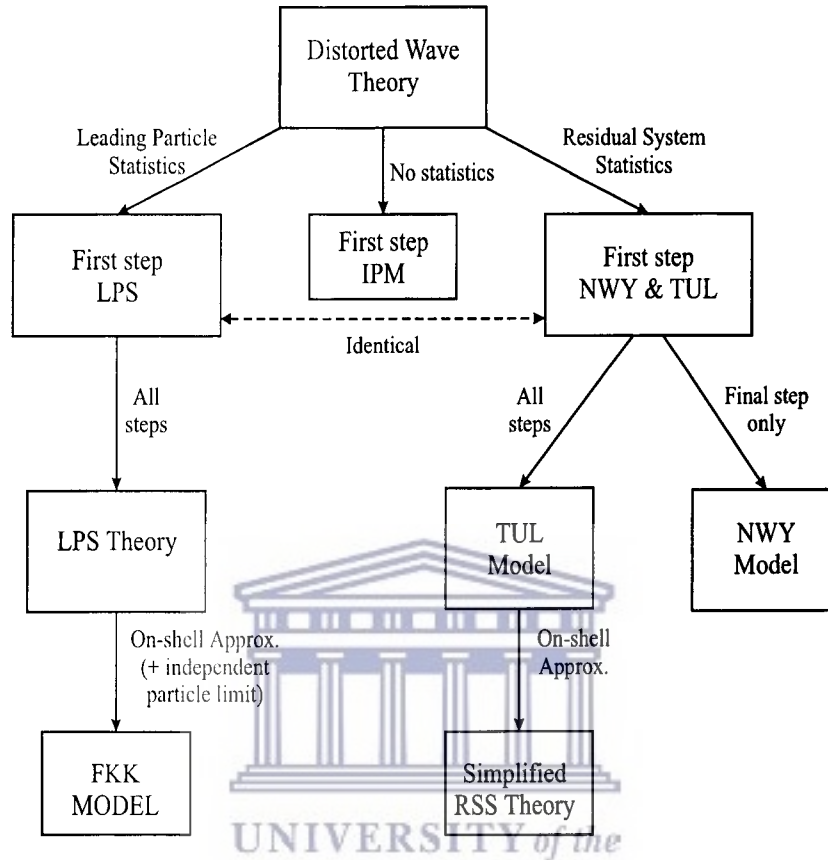


Figure 3.8: Relation between the various MSD theories.

The two types of statistics used are the leading particle statistics and residual system statistics. In leading particle statistics the interaction between the incident particle and the nucleus is modelled by V . It is also assumed that the incident particle can create many excited states within a certain energy interval. This in turn gives rise to matrix elements that vary in magnitude as well as in sign.

In residual system statistics, the interaction within the residual nucleus is given by H_1 of the complete Hamiltonian. Here we are looking at real nuclear states and assume that configuration mixing has a random character. This means that the coefficients $a_{m\mu}^n$ in the previous section assume random values.

3.4 The Double Differential cross-section

3.4.1 One Step cross-section

The main idea here is to use the energy-averaged DWBA cross-section in Eq. (3.26). With leading particle statistics all DWBA t-matrix elements have equal probability and the expression for the first-step becomes

$$\overline{\frac{d^2\sigma^{(1)}}{d\Omega dE_k}} = \rho_{m\mu}(E_x) \sum_{\mu} |\langle \chi^{(-)}(\mathbf{k}) | \langle 1\mu | V | 0 \rangle | \chi^{(+)}(\mathbf{k}_0) \rangle|^2. \quad (3.28)$$

The randomness approximation gives rise to the summing of individual transitions without interference. It is intuitively reasonable to expect that all transitions will not be equally likely. For example, a nucleus would rather undergo a 20 MeV excitation before it undergoes a 60 MeV excitation. The above expression becomes the following:

$$\overline{\frac{d^2\sigma^{(1)}}{d\Omega dE_k}} = \rho_{1p1h}(E_x) |\langle \chi^{(-)}(\mathbf{k}) | \langle 1p1h | V | 0 \rangle | \chi^{(+)}(\mathbf{k}_0) \rangle|^2, \quad (3.29)$$

where $\rho(E_k)$ is the particle-hole level density in the residual nucleus. The level density is usually evaluated with the Williams formula [19].

For the second step, using leading particle statistics, the following expression is obtained:

$$\begin{aligned} \overline{\frac{d^2\sigma^{(2)}}{d\Omega dE_k}} &= \sum_{\mu} \sum_{\nu} \int dE'_x \hat{\rho}_{1\mu}(E'_x) \hat{\rho}_{1\nu}(E''_x) \int d\mathbf{k}_1 \\ &\times |\langle \chi^{(-)}(\mathbf{k}) | \langle 1\nu | V | 0 \rangle | \chi^{(+)}(\mathbf{k}_1) \rangle \frac{1}{E - E'_x - E_{k_1} + i\epsilon} \\ &\times \langle \hat{\chi}^{(+)}(\mathbf{k}_1) | \langle 1\mu | V | 0 \rangle | \chi^{(+)}(\mathbf{k}_0) \rangle|^2. \end{aligned} \quad (3.30)$$

Now if we use the on-shell approximation, which corresponds to the conservation of energy during each step of the reaction, we get the following double-differential cross-section

$$\begin{aligned} \overline{\frac{d^2\sigma^{(2)}}{d\Omega dE_k}} &= \pi^2 \int d\mathbf{k}_1 \rho(k_1) \rho_{1p1h}(E''_x) \rho_{1p1h}(E'_x) \\ &\times \overline{|\langle \chi^{(-)}(\mathbf{k}) | \langle 1p1h | V | 0 \rangle | \chi^{(+)}(\mathbf{k}_1) \rangle|^2}^{1p1h} \\ &\times \overline{|\langle \hat{\chi}^{(+)}(\mathbf{k}_1) | \langle 1p1h | V | 0 \rangle | \chi^{(+)}(\mathbf{k}_0) \rangle|^2}^{1p1h}. \end{aligned} \quad (3.31)$$

3.5 MSD according to the FKK Theory

The FKK expressions for the evaluation of MSD cross-sections will now be given and explained. According to the FKK, the pre-equilibrium cross-section is given by the following expression

$$\left(\frac{d^2\sigma}{dU d\Omega}\right) = \left(\frac{d^2\sigma}{dU d\Omega}\right)_1 + \left(\frac{d^2\sigma}{dU d\Omega}\right)_M. \quad (3.32)$$

This expression depicts the importance of the first-step very clearly, since the first-step often constitutes most of the cross-section. The FKK theory equivalent of the Koning expression for the first-step cross-section is

$$\left(\frac{d^2\sigma}{dU d\Omega}\right)_1 = \sum_L (2L+1) \omega(U, L) \left\langle \left(\frac{d\sigma_1}{d\Omega}\right)_{DW} \right\rangle_L. \quad (3.33)$$

The form of this equation explicitly indicates the manner in which the double differential cross-section is evaluated. The last term in angle brackets denotes the average cross-section for all energetically possible $1p1h$ excitations corresponding to a particular angular momentum transfer. The term $\omega(U, L)$ is the density of particle-hole states in the residual nucleus.

The FKK expression for the multistep cross-section is as follows:

$$\begin{aligned} \left(\frac{d^2\sigma}{dU d\Omega}\right)_M &= \sum_n \sum_{m=n-1}^{n+1} \int \frac{d\mathbf{k}_1}{(2\pi)^3} \int \frac{d\mathbf{k}_2}{(2\pi)^3} \cdots \int \frac{d\mathbf{k}_n}{(2\pi)^3} \frac{d^2 W_{mn}(\mathbf{k}_f, \mathbf{k}_n)}{dU d\Omega} \\ &\times \frac{d^2 W_{n,n-1}(\mathbf{k}_n, \mathbf{k}_{n-1})}{dU_n d\Omega_n} \cdots \frac{d^2 W_{2,1}(\mathbf{k}_2, \mathbf{k}_1)}{dU_2 d\Omega_2} \left(\frac{d^2\sigma(\mathbf{k}_1, \mathbf{k}_i)}{dU d\Omega}\right)_1. \end{aligned} \quad (3.34)$$

This expression is nothing else but a folding of single transitions as in the Koning expression, which is a folding of two one-step transitions. The difference in these expressions is only in how they are calculated.

In the above equation the transition amplitude from the $(n-1)$ 'th stage to the n 'th stage is

$$\frac{d^2 W_{n,n-1}(\mathbf{k}_n, \mathbf{k}_{n-1})}{dU_n d\Omega_n} = 2\pi^2 \rho(\mathbf{k}_n) \rho_n(U) \langle |\nu_{n,n-1}(\mathbf{k}_n, \mathbf{k}_{n-1})|^2 \rangle, \quad (3.35)$$

where $\rho(\mathbf{k}_n)$ is the level density of the particles in the continuum, and $\rho_n(U)$ is the density of energy states of the particle-hole states in the residual nucleus as a function of excitation energy. The term $\nu_{n,n-1}$ is the matrix element for the transition while the particle in the continuum changes from momentum state k_{n-1} to state k_n .

The other points which pose some difficulties are the level density and the spin distribution parameters. In past and current calculations the level density is taken to be the same for all stages during the reaction and is evaluated with the Williams formula [19]

$$\rho_n(U) = \frac{g(gU)^{n-1}}{p!h!(n-1)!}, \quad (3.39)$$

where

p = the number of particles,

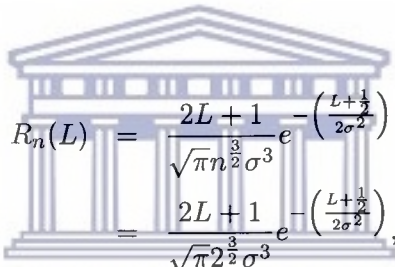
h = the number of holes,

n = number of particles and holes,

g = density of single-particle states, and

U = the excitation energy.

$n = 2$ for the MSD treatment, since $p = h = 1$. The spin distribution expression used is



$$R_n(L) = \frac{2L+1}{\sqrt{\pi n^{\frac{3}{2}} \sigma^3}} e^{-\left(\frac{L+\frac{1}{2}}{2\sigma^2}\right)} \quad (3.40)$$

$$= \frac{2L+1}{\sqrt{\pi 2^{\frac{3}{2}} \sigma^3}} e^{-\left(\frac{L+\frac{1}{2}}{2\sigma^2}\right)}, \quad (3.41)$$

where σ is the spin cut-off parameter from Gruppelaar *et al.* [33].

fitted data at slightly higher energies for (p, p') and (p, n) reactions, but still not reaching the 200 MeV region. As far as it is known, this work is the first attempt at fitting pre-equilibrium cross section data at 200 MeV while distinguishing between protons and neutrons and more importantly using a realistic N-N interaction.

4.1.1 The Effective Interaction

These calculations depend heavily on the DWBA cross-sections. The importance of the effective interaction can be seen directly through the DWBA T-matrix elements

$$T_{\beta\alpha}^{DWBA} = J \int d\mathbf{r}_\alpha \int d\mathbf{r}_\beta \chi_\beta^{(-)*}(\mathbf{k}_\beta, \mathbf{r}_\beta) (\Phi_B \Phi_b | V_\beta - U_\beta | \Phi_A \Phi_a) \chi_\alpha^{(+)}(\mathbf{k}_\alpha, \mathbf{r}_\alpha), \quad (4.1)$$

where the term of importance is $(\Phi_B \Phi_b | V_\beta - U_\beta | \Phi_A \Phi_a)$. This term written more explicitly is $(\Phi_B \Phi_b | V_{eff} | \Phi_A \Phi_a)$ and it determines the strength of the transition from the initial to the final nuclear state. By implementing the Yukawa potential, the physics behind this transition process is obscured by the simplicity of the interaction. This has the implication that even if one should observe any new phenomena, one would be unable to ascribe the result to any real physical process.

Let us now consider the effective interaction in more detail. The Yukawa interaction does not take into account the effects due to spin and isospin of the interacting particles. It can be shown that the most general form of the effective interaction [21, 25, 29] including spin and isospin can be written as

$$V_{eff}(r, \vec{\sigma}_1, \vec{\sigma}_2, \vec{\tau}_1, \vec{\tau}_2) = V^C(r) + V^{SO}(r) + V^{Ten}(r). \quad (4.2)$$

The first term on the right-hand side is the central interaction, the second the spin-orbit and the third, the tensor interaction. $\vec{\sigma}_1$ and $\vec{\sigma}_2$ are the Pauli spin operators for interacting particles, in this case labelled **1** and **2**.

The isospin for a nucleon is one-half, with projections of $T_z = \frac{1}{2}$ for a proton and $T_z = -\frac{1}{2}$ for a neutron. The possible two-nucleon isospin states are thus $T = 0$ (isospin singlet) and $T = 1$ (isospin triplet). The possible projections are $T_z = 1$, corresponding to a proton-proton (p-p) system, $T_z = 0$, corresponding to a proton-neutron (p-n) system and $T_z = -1$, corresponding to a neutron-neutron (n-n) system. $T = 0$ refers exclusively to a p-n system, while $T = 1$, could be a p-p, a p-n or an n-n system [16].

The possible two-nucleon systems that are allowed in accordance with the Pauli exclusion principle are shown in the table below.

Table 4.1: Allowed two-nucleon states.

Two-nucleon System	Total Spin S	Total Isospin T	Allowed Angular Momentum Value (Positive integer)
p-p	0	1	Even
p-p	1	1	Odd
n-n	0	1	Even
n-n	1	1	Odd
p-n	0	1	Even
p-n	1	1	Odd
p-n	0	0	Odd
p-n	1	0	Even

The central interaction is regarded as the most important part of the interaction [28]. The significance of the spin-orbit and the tensor interaction only becomes appreciable for large angular momentum transfers. In these MSD calculations the lower angular momentum transfers do contribute more to the overall cross-section for the first step. It is for this reason that the central interaction will be considered in more detail than the spin-orbit and the tensor interaction.

Writing out the expression for the central component we get

$$V^C(r) = V_{00}(r) + V_{01}(r)(\vec{\tau}_1 \cdot \vec{\tau}_2) + [V_{10}(r) + V_{11}(r)(\vec{\tau}_1 \cdot \vec{\tau}_2)](\vec{\sigma}_1 \cdot \vec{\sigma}_2). \quad (4.6)$$

The composition of the central interaction for various spin and isospin possibilities can be

4.1.2 Differentiating between particle-hole types.

The second aspect included in the MSD calculations in this work, considers how the (p, p') reaction takes place in terms of particle-hole excitations. The different ways of getting the p' for the reaction is shown Fig. 4.1, as well as for the (p, n) reaction which can contribute to (p, p') in the second step.

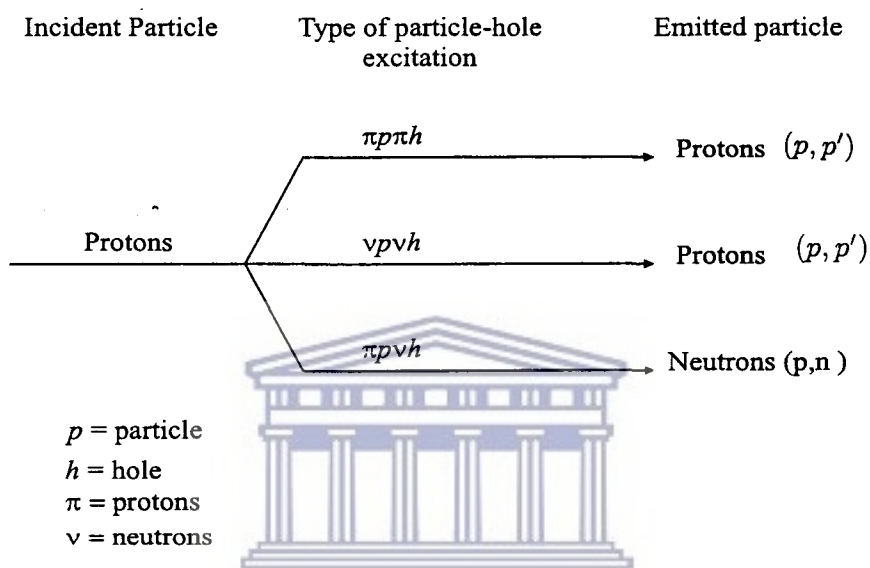


Figure 4.1: First-step processes.

All these output cross-sections are required in the multistep calculation. It is clear that the cross-section for the (p, p') is now calculated differently than before.

The calculation involves two main processes, which are depicted by Part I and Part II respectively. Part I is the calculation of the associated DWBA cross sections, while Part II is the calculation of the pre-equilibrium cross section. Apart from a few modifications, this code is identical to the code sequence used by [3]. Most of the details regarding this sequence can be found in [3] and other references therein. The emphasis here will be on the modifications made to investigate possible calculational improvements.

MSIW.exe

MSIW.EXE generates the possible transitions using the spherical Nilsson model [11] for the nucleus. Nuclear transitions are dictated by the conservation of angular momentum and energy. Despite this, the number of possible ways in which the nucleus may be excited is still large. It is for this reason that this program selects the possible excitations in terms of a specific excitation energy and angular momentum transfer. In our case five different energy bins are used. The minimum excitation energy being 20 MeV and the maximum 100 MeV, since the effective interaction is only expected to be valid at incident energies above 100 MeV. Each bin corresponds to a specific excitation energy. Bin 1 corresponds to 20 MeV excitations. It contains all possible transitions in which case the excitation energy is between 10 and 30 MeV. The details of the energy bins are given in the table below.

Table 4.3: Energy bin details.

Bin Number	Excitation Energy Range (MeV)	Excitation Energy (MeV)
1	10 - 30	20
2	30 - 50	40
3	50 - 70	60
4	70 - 90	80
5	90 - 110	100

In each bin the possible angular momentum transferred ranges from zero to a maximum of ten. Usually [28] the maximum angular momentum transfer of importance does not have to exceed eight. The output of MSIW.EXE is written to the files with the .CNF extension. A sample file is shown in the appendix.

In the work by Steyn [3], no distinction was made between proton particle-hole and neutron particle-hole excitations and particle-hole excitations originating from the (p, n) reaction. For

4.3 Calculational Details and Results

As mentioned earlier, the aim of this work is to use a more realistic effective interaction for the calculation of pre-equilibrium cross-sections. Not only does this require a model for the effective interaction (Amos interaction), but also a computer code

Four calculations are performed, the first of which is a comparison of computational results obtained from using the Yukawa function as the effective interaction, in DW91N and DWUCK respectively.

The second calculation is the comparison of the computational results obtained from using the Amos interaction and the measured data. The results obtained from the Yukawa interaction are also presented. Calculations three and four are attempts at improvin

Calculation 1: Comparison of DW91N and DWUCK.

The reason for performing this calculation, is that most calculations of this type have used the Yukawa as the effective interaction. The Yukawa is phenomenological in nature and has the form

$$V(r) = V_0 \frac{e^{-\mu r}}{\mu r}, \quad (4.9)$$

where V_0 is the effective interaction strength and μ the inverse of the interaction range. The main input parameters in the calculation are the interaction strength, V_0 , the level density and the spin cut-off parameter. In DW91N, the value for V_0 is taken in accordance with the interaction strength chosen in past calculations [28]. The level density parameter is chosen in accordance with the prediction by Shlomo [31]. The results from using DWUCK as the DWBA cross-section code, are taken from the work by Steyn [3]. The parameters used in this work are tabulated in Table 4.4.

Table 4.4: Level density and spin cut-off values.

Code	V_0	a	σ
DW91N	25 MeV	9.71	3.1
DWUCK	15 MeV	10.68	3.6

Since the V_0 value used by Steyn differs from that used in DW91N, the results for DWUCK

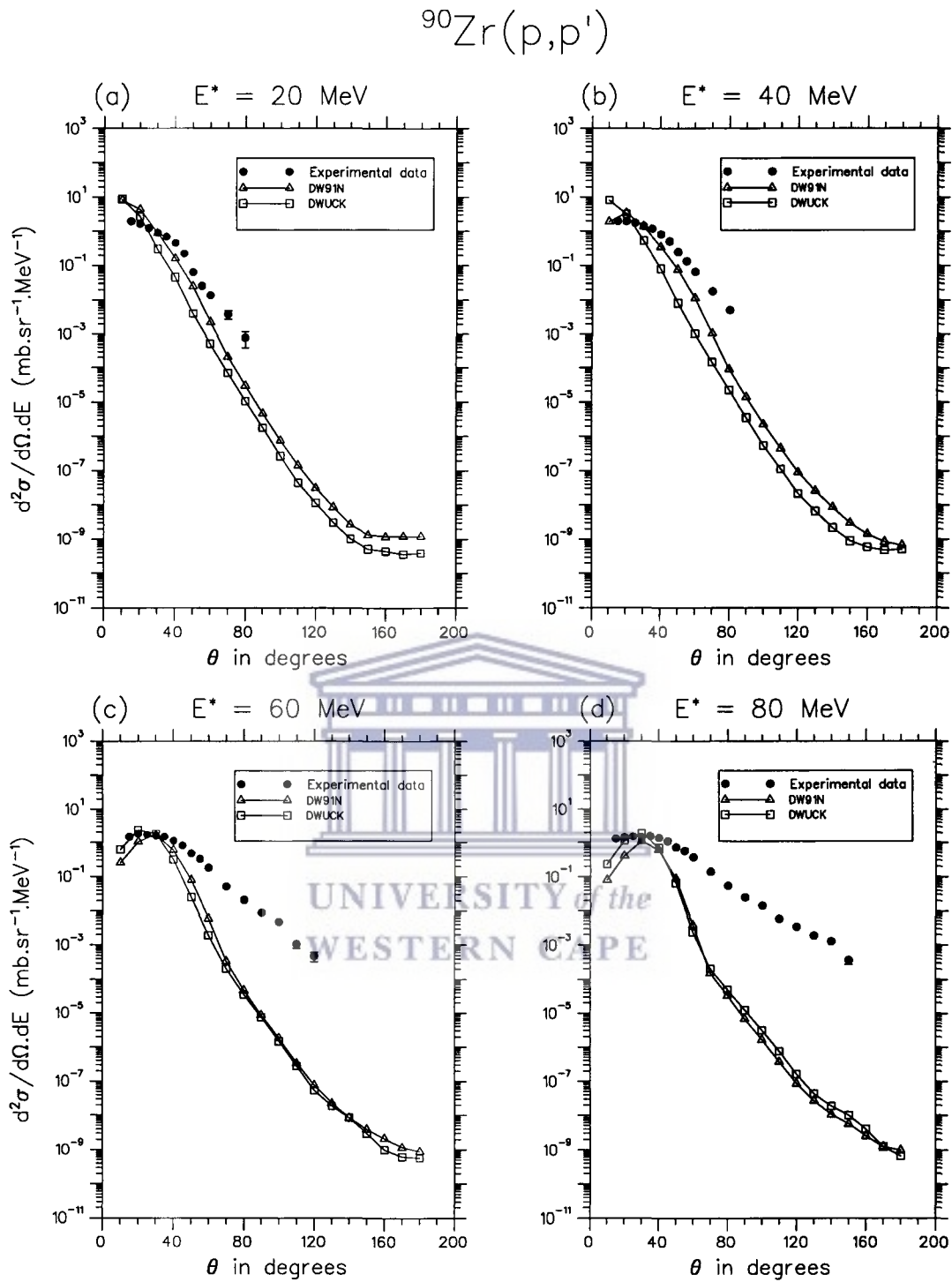


Figure 4.3: Comparison between DW91N and DWUCK with a Yukawa interaction. E^* denotes excitation energy.

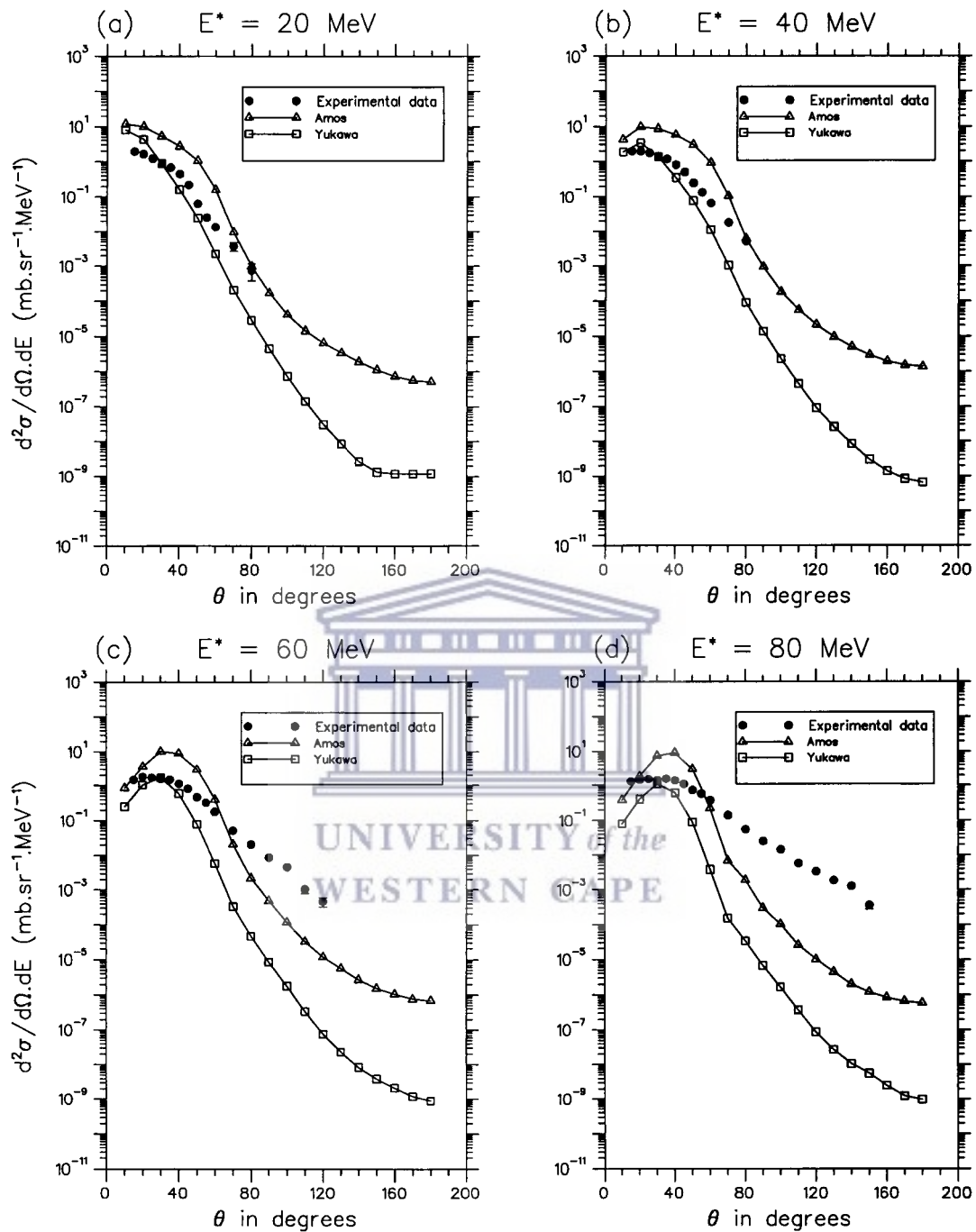
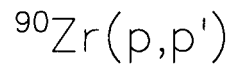


Figure 4.4: The Amos interaction results compared with Yukawa interaction results from DW91N.

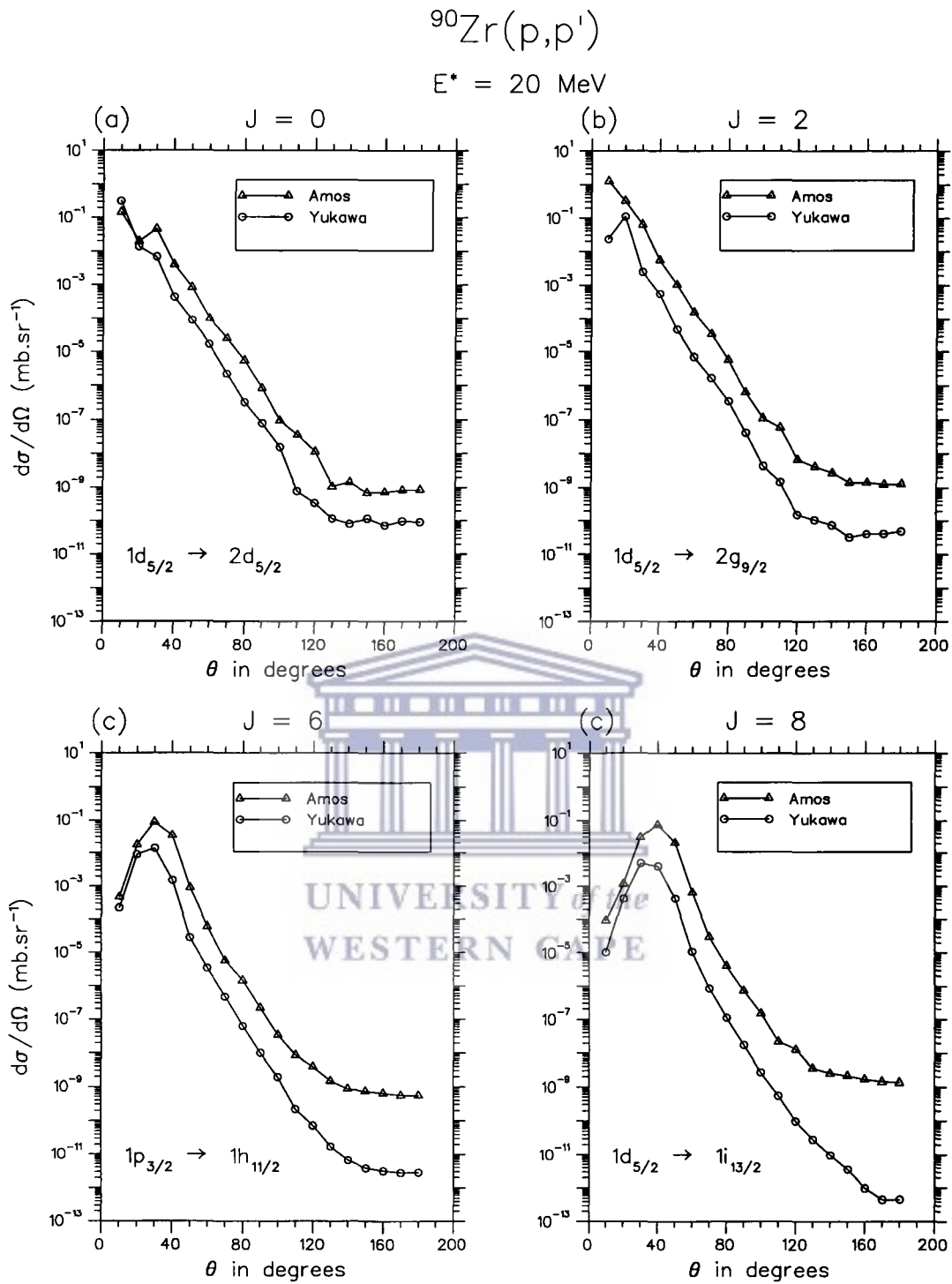


Figure 4.6: Individual DWBA cross-sections for the Amos interaction. 20 MeV excitation for $J = 0, 2, 6$ and 8 for Amos and Yukawa interactions for protons.

The two calculations are now presented which attempt to solve the overprediction of the cross-section. Both calculations are identical to **calculation 2**, but differ with respect to the allowed particle-hole excitations.

Calculation 3: Removal of low-lying states.

In this calculation the particle-hole excitations, where the hole is created at very low-lying states, are ignored.

If one considers direct processes to occur mainly at the nuclear surface [29] and the assumption that nucleons in lower shells are less likely to be at the surface, one would expect the N-N interaction to be primarily between the incident nucleon and the outer shell nucleons. This calculation tests the reduction in cross-section prediction when transitions originating below the $1f_{7/2}$ -shell are removed from the .CNF file. The $1f_{7/2}$ -shell is the first shell after the third shell closure. Hence the assumption here is that the the lowest three major shells are inert and do not contribute to pre-equilibrium scattering. A schematic picture of the ^{90}Zr shell structure is shown below. One can see that the number of nucleons which can now be excited are considerably less.

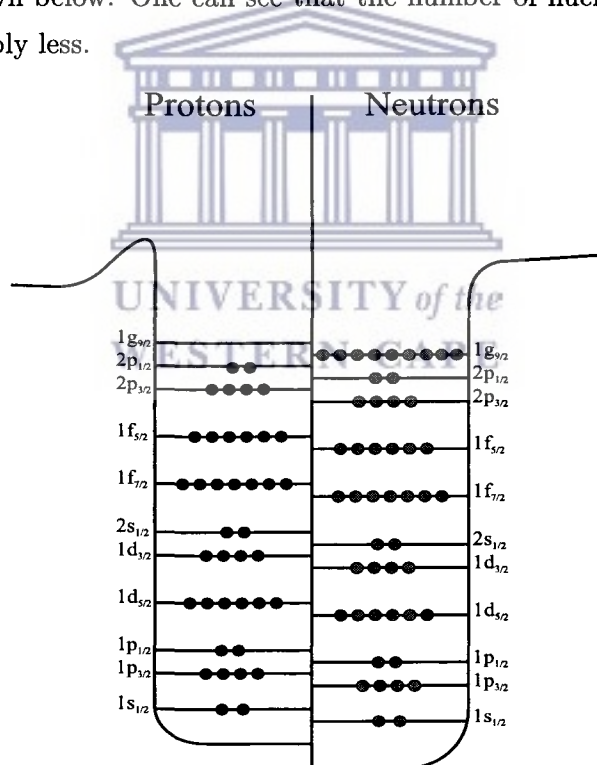


Figure 4.8: Shell structure for ^{90}Zr .

Calculation 4: Removal of higher energy shell model states.

In this calculation only particle-hole transitions that terminate in bound nuclear shells are included in the .CNF file. The bound shells were determined from a Hartree-Fock calculation by employing a Skyrme interaction [21]. The highest bound shell for protons are taken to be the $2d_{3/2}$ -shell and for neutrons the $1h_{11/2}$ -shell. The results for this calculation are shown in Fig. 4.10.

Fig. 4.10 shows that this calculation results in a considerable reduction in the cross-section predictions. However, the cross-section for the first two bins (see Table 4.3) still overpredict the data at low angles, even though this is still only

This calculation shows that the inclusion of unbound levels in the possible transitions makes an important difference and that an improved nuclear structure model for the target nucleus should be investigated further.

The results in this chapter pose a challenge to the field of quantum mechanical descriptions of pre-equilibrium cross-sections using the FKK formalism. The use of a realistic effective interaction used in this work, which has been successfully applied in elastic and inelastic scattering to discrete states, overpredicts the cross-section substantially at low angles, even when only the first-step is included. There is some indication that an improved nuclear model will be required, but this needs further investigation.

Chapter 5

Conclusion

The first-step pre-equilibrium cross-section for the reaction of 200 MeV protons on ^{90}Zr have been calculated with a more realistic effective interaction [6]. The effective interaction used is the Amos interaction, which replaces the Yukawa potential. These calculations are based on the multistep direct theory of Feshbach, Kerman and Koonin [5]. Implementation of the theory is achieved by expressing the multistep cross-section as a folding of DWBA cross-sections. The multistep calculation is implemented in the MSD code by Bonetti [7], which has also been modified to distinguish between protons and neutrons in the calculation of the different steps. Also new to these calculations is the implementation of DW91N by Raynal [30], a DWBA code similar to DWUCK [35]. The difference between these two codes is that DW91N can use a better effective interaction.

The two DWBA codes were compared for purposes of consistency and a good agreement between the respective results were obtained. There were slight differences for the lower excitation energies (Fig. 4.3(a) and (b)), but these are thought to arise from the factor of $(2j + 1)$, which has been omitted from the DWUCK calculation.

The implementation of the Amos interaction generally shows an overprediction of the cross-section. The overprediction of the cross-section arises from the overpredicted (Fig.4.6 and 4.7) DWBA cross-sections when compared to the Yukawa interaction. Various attempts have been made to explain the overprediction of the data by the first step. The subsequent calculations are based on changing the number and type of nuclear transitions for nuclear



UNIVERSITY *of the*
WESTERN CAPE

Table A.1: Sample .CNF file

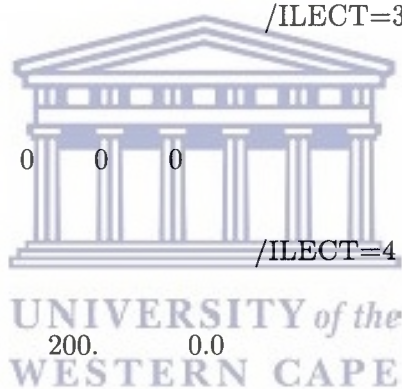
L_{tr}	E_{bin}	n	ℓ	$2j$	n'	ℓ'	$2j'$	E_{ex}
0	1	0	2	5	1	2	5	16.94
0	2	0	0	1	2	0	1	49.50
0	4	0	0	1	3	0	1	75.00
1	1	0	1	3	1	2	5	26.24
1	2	1	1	1	2	2	3	32.75
1	3	0	0	1	2	1	3	64.39
2	1	0	2	5	0	4	9	11.63
2	2	0	0	1	1	2	5	48.57
2	4	0	0	1	2	2	5	72.58
3	1	0	1	3	0	4	9	20.94
3	2	0	1	3	1	4	9	46.53
3	3	0	0	1	1	3	7	53.50
4	1	0	1	3	0	5	11	27.92
4	2	0	0	1	0	4	9	43.27
4	3	0	0	1	1	4	9	68.86
5	1	0	1	3	0	4	9	20.94
5	2	0	1	3	0	6	13	32.85
5	3	0	0	1	0	5	11	50.25
5	4	0	0	1	1	5	11	77.23
6	1	0	1	3	0	5	11	27.92
6	2	0	1	3	0	5	9	32.57
6	3	0	0	1	0	6	13	55.18
6	4	0	0	1	0	6	11	71.09
7	1	0	2	5	0	5	11	18.61
7	2	0	1	3	0	6	13	32.85
7	3	0	0	1	0	7	15	69.79
8	1	0	2	5	0	6	13	23.54
8	2	0	1	3	0	7	15	47.46
9	1	0	3	7	0	6	13	16.56
9	1	0	3	5	0	6	13	13.31
9	2	0	3	7	0	6	11	32.47
10	1	0	3	5	0	7	15	27.92

Figure A.1: Sample .MDS91 file.

```

11 5 1 7 2 13
0 1 2 3 4 5 6 7 8 9 10
100.0 120.0 140.0 160.0 180.0
1.0 40. 1. 40. -8. -8.
C ZR-90 200MeV proton p-h state zr-pppp1200.ms91
FTFFFFT
1 /ILECT=1
200 2 1
.08 90.
FTFF
90.0 39.0 1.25 1.2 0.6 0.0
0.0 0.6 0.0 0.0
2 /ILECT=2
3 /ILECT=3
18 60 40 0 6
10.0 180.
0 0 0 0 0 0 0 0
F
4 /ILECT=4
FFFFF
90.0 1.00 40.0 200. 0.0
1.25
5 /ILECT=5
FFFFFF
90.0 1.00 40.0 200. 0.0
1.25
6 /ILECT=6
2 +1 1
FFFFFF
+1.0 1.0
2 1
7 /ILECT=7
END

```



A.3 *.DW91* input file.

Table A.2 shows a partial input file for DW91N.EXE, containing only the 80 MeV excitation portion. Each /ILECT contains the information as in the previous .MSD91 file, but this time all the details of the calculation are included. Of particular interest is /ILECT 1, which shows three .CNF states along with their optical potentials. Transitions are among the list of about 29 transitions of this nature. /ILECT 6 contains the actual calculations performed, followed by /ILECT 7 to terminate each calculation.



3 /ilect 3
 18 60 40 0 6
 10.00000 180.00000
 0 0 0 0 0 0 0 0

F

4 /ilect 4

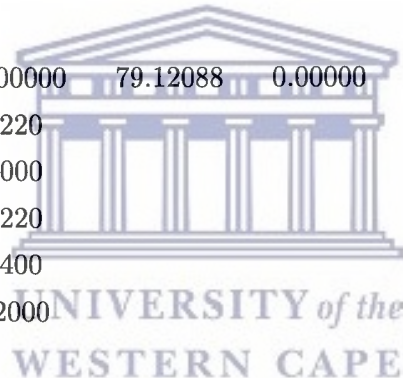
FFFFF

90.00000 1.00000 40.00000 200.00000 0.00000
 16.50031 1.25500 0.73700
 16.56336 1.17000 0.82000
 0.000000 1.25500 0.73700
 1.872440 1.05666 0.60000
 -2.35487 1.03831 0.62000
 1.25000

5 /ilect 5

FFFFFFF

90.00000 1.00000 40.00000 79.12088 0.00000
 25.25777 1.24500 0.71220
 7.939680 1.36200 0.62000
 0.000000 1.24500 0.71220
 3.483580 1.05666 0.62400
 -1.40473 1.03831 0.62000
 1.25000



6 /ilect 6

0 1 1

FFFFFFF

1.00000 1.00000 0.00000
 2 1
 1.00000 0.00000

7 /ilect 7

C ZR-90 200MeV proton p-h state zr-pppp1200.msd91

FTFFFFFFT

6 /ilect 6

2 1 1

A.4 .MUDIR file

Line 1 = Title card.

Line 2

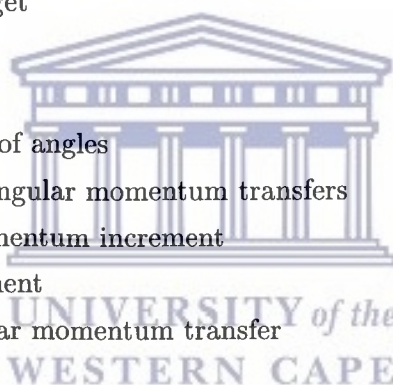
90. = mass of the target
 200. = incident energy of the proton
 7.094,7.094 = binding energy of the incident and exit particle respectively
 10.6 = level density
 0.0 = pairing energy
 20.,20. = width of energy bins and the size of the first excitation.

Line 3

3.105 = spin cut-off parameter
 40. = Z of the target

Line 5

18 = the number of angles
 11 = number of angular momentum transfers
 1 = angular momentum increment
 10 = angle increment
 0 = initial angular momentum transfer



Line 6 - 10 = the transitions according to bin and angular momentum transfer for neutron-particle and neutron-hole excitations. Line 6 corresponds to bin 5 (100 Mev excitation) and line 10 to bin 1 (20 MeV excitation).

Line 11 - 15 = the same as above, but for proton particle - proton hole excitations.

Line 17 - 21 = same as above, but for proton particle - neutron hole excitations.



UNIVERSITY *of the*
WESTERN CAPE

- [12] P. E. Hodgson, Workshop on Applied Nuclear Theory and Nuclear Model Calculations for the Nuclear Technology Applications, Trieste, Italy, 15 Feb - 19 Mar 1988, *Editors* M. K. Mehta and J. J. Schmidt, World Scientific, 1989.
- [13] N. K. Glendenning, *Direct Nuclear Reactions*, Academic Press, 1983.
- [14] Monte Carlo N-Particle Transport Code System, Oak Ridge National Laboratory.
- [15] K. S. Krane, *Introductory Nuclear Physics*, John Wiley and Sons Inc., 1988.
- [16] A. E. S. Green, T. Sawada, D. S. Saxon, *The Nuclear Independent Particle Model*, Academic Press, 1968.
- [17] G. Arfken, *Mathematical Methods for Physicists*, Academic Press Inc., 1985.
- [18] N. Austern, *Direct Nuclear Reaction Theories*, John Wiley and Sons, Inc. 1970.
- [19] E. Gadioli and P. E. Hodgson, *Pre-Equilibrium Nuclear Reactions*, Clarendon Press, Oxford, 1992.
- [20] H. Feshbach, *Theoretical Nuclear Physics - Nuclear Reactions*, John Wiley and Sons, Inc., 1992.
- [21] P. J. Siemens and A. S. Jensen, *Elements of Nuclei - Many Body Physics with the strong interaction*, Addison-Wesley Publishing Company, Inc., 1987.
- [22] D. F. Jackson, *Nuclear Reactions*, Nederlandse Boekdrukk Industrie, 1970.
- [23] A. Koning, *Multi-Step Direct Reactions*, PhD Thesis, Rijksuniversiteit Groningen, 1992.
- [24] M. A. Preston and R. K. Bhaduri, *Structure of the Nucleus*, Addison-Wesley Publishing Company Inc., 1975.
- [25] P. Ring and P. Schuck, *The Nuclear Many-Body Problem*, Springer-Verlag Inc., 1980.
- [26] R. Lindsay, "The use of effective interactions in Pre-Equilibrium Reactions, International Symposium on Pre-Equilibrium Reactions", Smolenice Castle, 23-27 October, 1995.
- [27] M. B. Chadwick, R. Bonetti and P. E. Hodgson, *J. Phys. G* **15**, 237 (1989).
- [28] S. M. Austin, in *The (p,n) Reaction and the Nucleon-Nucleon Force*, edited by C. D. Goodman *et al.*, (Plenum, New York, 1980), p. 203.